Controllable Fast and Slow Light in the Hybrid Nanomechanical Resonator System

Hua-Jun Chen (chenphysics@126.com)
Anhui University of Science and Technology

Nano Express

Keywords: nanomechanical resonator, Fano resonance, slow light, fast light

Posted Date: June 8th, 2021

DOI: https://doi.org/10.21203/rs.3.rs-559903/v1

Controllable fast and slow light in the hybrid nanomechanical resonator system

Hua-Jun Chen

School of Mechanics and Photoelectric Physics, Anhui University of Science and Technology, Huainan Anhui 232001, China
**chenphysics@126.com*

Abstract: We propose a hybrid nanomechanical resonator (NR) system, where a NR coupled to an embedded quantum dot (QD) driven by two-tone fields is also coupled to another NR via the Coulomb interaction, and investigate the absorption spectra of the probe field under both the condition of resonance and off-resonance. The absorption spectra in resonance presents a means to determine the coupling strength of the two NRs. In the off-resonance, the absorption spectra can exhibit double Fano resonance, and the positions of the double Fano resonances are related to the interaction of the two NRs, the frequencies of the NRs, and the pump detuning. Furthermore, the double Fano resonances are accompanied by the rapid normal phase dispersion, which indicates the slow- and fast-light effect. We can obtain that the group velocity index is tunable by the interaction between the two NRs, the detuning, and the different resonator frequencies, which can reach the conversion from the fast light to slow light.

keywords: nanomechanical resonator; Fano resonance; slow light; fast light

1. Introduction

In the past few decades, many techniques and progresses have been proposed to reach the fast- and slow-light in atomic vapors and solid-state devices, which need to control the group velocity index n_g of light pulses and make them propagate either $n_g < 0$ (i.e., the fast light) or $n_g > 0$ (i.e., the slow light) [1, 2]. To obtain the manipulation of light pulse propagation in different systems, lots of techniques have been developed, such as the famous electromagnetically induced transparency technologies [3–5], the stimulated Brillouin scattering schemes [6, 7], the coherent population oscillation in solid-state devices [8], and the Fano-like resonance phenomena [9–12]. Here, in this paper, we investigate the tunable and controllable fast light and slow light in hybrid NR systems, which is mediated by another NR.

NR systems, due to their high natural frequencies and large quality factors [13], are applied to different applications such as the detection of mechanical signal [14], mass sensors [15, 16], mechanical displacements measurements [17], and spin detecting [18]. Additionally, recent progress in nanotechnology has allowed the fabrication of novel hybrid systems including a single two-level system (TLS) coupled to a NR [19–23], in which the quantum nature can be revealed and manipulated [24]. These hybrid NR systems indicate underlying applications quantum information technologies [25], as well as the exploration of the quantum-classical boundary. As a representative hybrid system, a two-level QDs coupled to a NR has attracts much interest [26–28], which can be used to investigate the fundamental quantum effects [29], high precision measurement [30], zeptogramscale mass sensing [31], and cooling of a NR to its quantum ground state [26].

In the previous NR systems, only one NR coupled to a TLS QD is considered, here, we develop the single NR system and introduce another NR with the interaction λ_1 between the two NRs, where the interaction strength λ_1 can be realized via a substrate-mediated

interaction [32] or the Coulomb interaction [33–35]. As shown in Fig.1, we propose a hybrid NRs system, where a doubly clamped suspended NR with an embedded QD driven by two-tone fields couples to another NR via Coulomb interaction. We first investigate the probe absorption spectra of the QD under the condition of resonance for different coupling strengths of the two NRs with the same resonator frequencies, which presents a means to determine the coupling strengths of the two NRs.

In the coherent optical propagation, Fano resonances are characterized by a rapid steeper dispersion than conventional Lorentzian resonances, which promises the slow- or fast-light effect, and even tunable fast-to-slow light propagation (or vice versa). In the off-resonance, the absorption the QD induced by the coupling of the NRs are also demonstrated, where the slope of the dispersion experiences the conversion from negative to positive, and the absorption displays the asymmetric Fano line shapes. The Fano resonances can be effectively tuned and the probe absorption spectra can display a series of asymmetric Fano line shapes with tuning the detuning. Due to Fano resonances are characterized by a rapid steeper dispersion, the group velocity index n_g of light pulses can be accelerated and decreased significantly, which correspond to the negative and positive dispersion, respectively. Then, we further investigate the slow light effect by numerically calculating the group delay of the probe field around the transparency window accompanied by the steep phase dispersion, and we find a tunable and controllable fast-to-slow light propagation (and vice versa) can be achieved with manipulating the parameter regimes. However, the tunable slow and fast light phenomenon in our system is different from the previous NR system [36] which depends on the incident pump laser is on- and off-resonant with the exciton frequency, here, in our hybrid NRs system, we can obtain the conversion from fast to slow light by controlling the coupling between different NRs.

2. System and Model

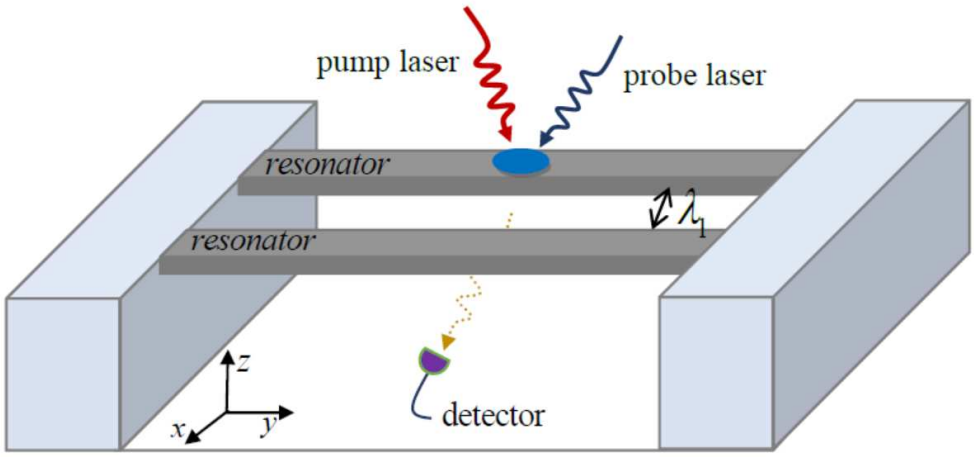

Fig. 1. Schematic diagram of hybrid hybrid nanomechanical resonator (NR) system, where a doubly clamped suspended NR (with frequency ω_{m1}) with an embedded QD driven by two-tone fields is coupled to another NR (with frequency ω_{m2}) via the Coulomb interaction with coupling strengths λ_1.

The system under consideration is sketched in Fig. 1, where a QD driven by a strong pump field and a weak probe field is embedded in a NR with frequency ω_{m1} is coupled to another NR with frequencies ω_{m2}, and the Hamiltonian of the hybrid system is given by [26, 35–38]

$$H = \hbar\omega_{ex}S^z + \hbar\omega_{m1}a_1^\dagger a_1 + \hbar\omega_{m2}a_2^\dagger a_2 + \hbar\omega_{m1}\beta S^z(a_1^\dagger + a_1) + \hbar\lambda_1(a_1^\dagger a_2 + a_1 a_2^\dagger) - \mu\varepsilon_p(S^+e^{-i\omega_p t} + S^-e^{i\omega_p t}) - \mu\varepsilon_s(S^+e^{-i\omega_s t} + S^-e^{i\omega_s t}) \quad (1)$$

where the first term indicates the Hamiltonian of the QD with the exciton frequency ω_{ex}. Here we consider the QD is a TLS including the ground state $|0\rangle$ and the single exciton state $|1\rangle$ [39, 40] at low temperature, and we introduce the pseudospin operators S^z and $S^\pm$ to describe the TLS QD. The second and third terms indicate the free Hamiltonian of the two NRs and we use creation (annihilation) operators $a_1^\dagger(a_1)$ and $a_2^\dagger(a_2)$ to describe the two NRs. The fourth term shows the coupling between the NR and QD with the coupling strength β, where the flexion induces extensions and compressions in the structure, and the longitudinal strain will modify the energy of the electronic states of QD through deformation potential coupling. The fifth term means the interaction between the NRs with strength λ_1, which be realized via a substrate-mediated interaction [32] or the Coulomb interaction [33–35]. The last two terms in Eq. (1) indicate the interactions between the QD and two laser fields including a strong pump field (with frequency ω_p) and a weak probe field (with frequency ω_s) simultaneously driving the QD, where μ is the electric dipole moment of the exciton, ε_p and ε_s are the slowly varying envelope of the pump field and probe field, respectively. When we use a rotating frame at the pump frequency ω_p, then Eq. (1) can be rewritten as

$$H = \hbar\Delta_p S^z + \hbar\omega_{m1}a_1^\dagger a_1 + \hbar\omega_{m2}a_2^\dagger a_2 + \hbar\omega_{m1}\beta S^z(a_1^\dagger + a_1) + \hbar\lambda_1(a_1^\dagger a_2 + a_1 a_2^\dagger) - \hbar\Omega_p(S^+ + S^-) - \mu\varepsilon_s(S^+e^{-i\delta t} + S^-e^{i\delta t}) \quad (2)$$

with the exciton-pump field detuning $\Delta_p = \omega_{ex} - \omega_p$, the probe-pump detuning $\delta = \omega_s - \omega_p$, and the Rabi frequency of the pump field $\Omega_p = \mu\Omega_p/\hbar$. Then we can obtain the following Heisenberg equations of the operators [41]:

$$\partial_t S^z = -\Gamma_1(S^z + 1/2) + i\Omega_p(S^+ - S^-) + \frac{i\mu\varepsilon_s}{\hbar}(S^+e^{-i\delta t} - S^-e^{i\delta t}) \quad (3)$$

$$\partial_t S^- = -(i\Delta_p + \Gamma_2)S^- - i\omega_{m1}\beta X_1 S^- - 2i\Omega_p S^z - \frac{2i\mu\varepsilon_s S^z}{\hbar}e^{-i\delta t} + \iota_{in} \quad (4)$$

$$\partial_t^2 X_1 + \gamma_{m1}\partial_t X_1 + \omega'^2_{m1} X_1 + \lambda' X_2 = -2\omega_{m1}^2\beta S^z + \xi_1 \quad (5)$$

$$\partial_t^2 X_2 + \gamma_{m2}\partial_t X_2 + \omega'^2_{m2} X_2 + \lambda' X_1 = -2\lambda\omega_{m1}\beta S^z + \xi_2 \quad (6)$$

where $\Gamma_1(\Gamma_2)$ is the exciton relaxation rate (dephasing rate), γ_{m1} and γ_{m2} are the decay rate of the two NRs. $\omega'^2_{m1} = \omega_{m1}^2 + \lambda_1^2$, $\omega'^2_{m2} = \omega_{m2}^2 + \lambda_1^2$, $\lambda' = \lambda_1(\omega_{m1} + \omega_{m2})$. ι_{in} in is the δ -correlated Langevin noise operator with zero mean, and ξ_k is Langevin force arising from the interaction between the kth mechanical resonator and its environment.

Using $\rho = \rho_0 + \delta\rho$ (ρ indicates the operators: S^z, S^-, X_1, X_2), Eqs. (3)-(6) can be divided into the steady parts and the fluctuation ones. Substituting the division forms into Eqs. (3)-(6), we obtain the steady state solutions of the variables as follows,

$$\Gamma_1(\omega_0 + 1) = 2i\Omega_p(S_0^* - S_0) \quad (7)$$

$$(i\Delta_p + \Gamma_2)S^0 + i\omega_{m1}\beta X_{10}S_0 = -i\omega_0\Omega_p \quad (8)$$

$$\omega'^2_{m1} X_{10} + \lambda' X_{20} = -\omega_0\omega_{m1}^2\beta \quad (9)$$

$$\omega'^2_{m2} X_{20} + \lambda' X_{10} = -\omega_0\lambda\omega_{m1}\beta \quad (10)$$

which determine the population inversion ($\omega_0 = 2S_0^z$) of the exciton. Due to the pump field is strong, the operators can use their expectation values with the mean-field approximation $\langle Qc\rangle = \langle Q\rangle\langle c\rangle$ [42]. After being linearized by neglecting nonlinear terms in the fluctuations, the Langevin equations for the expectation values can be obtain as follows:

$$\langle \partial_t \delta S^z \rangle = -\Gamma_1 \langle \delta S^z \rangle + i\Omega_p (\langle \delta S^+ \rangle - \langle \delta S^- \rangle) + \frac{i\mu\varepsilon_s}{\hbar}(S_0^* e^{-i\delta t} - S_0 e^{i\delta t}) \tag{11}$$

$$\langle \partial_t \delta S^- \rangle = -(i\Delta_p^{'} + \Gamma_2)\langle \delta S^- \rangle - i\omega_{m1}\beta S_0 \langle \delta X_1 \rangle - 2i\Omega_p \langle \delta S^z \rangle - \frac{i\mu\varepsilon_s \omega_0}{\hbar} e^{-i\delta t} \tag{12}$$

$$\langle \partial_t^2 \delta X_1 \rangle + \gamma_{m1} \langle \partial_t \delta X_1 \rangle + \omega_{m1}^{'2} \langle \delta X_1 \rangle + \lambda^{'} \langle \delta X_2 \rangle = -2\omega_{m1}^2 \beta \langle \delta S^z \rangle \tag{13}$$

$$\langle \partial_t^2 \delta X_2 \rangle + \gamma_{m2} \langle \partial_t \delta X_2 \rangle + \omega_{m2}^{'2} \langle \delta X_2 \rangle + \lambda^{'} \langle \delta X_1 \rangle = -2\lambda\omega_{m1}\beta \langle \delta S^z \rangle \tag{14}$$

where $\Delta_p^{'} = \Delta_p + \omega_{m1}\beta\omega_0\alpha$ and $\alpha = \dfrac{\omega_{m1}\beta(\lambda^{'}\lambda - \omega_{m1}\omega_{m2}^{'2})}{\omega_{m1}^{'2}\omega_{m2}^{'2} - \lambda^{'2}}$.

To solve these equations, we make the ansatz [43] as $\langle \delta\rho \rangle = \rho_+ e^{-i\delta t} + \rho_- e^{i\delta t}$, and substituting them into Eqs. (11)-(14) with ignoring the second-order terms and working to the lowest order in ε_s but to all orders in ε_p , we obtain the linear optical susceptibility as $\chi_{eff}^{(1)}(\omega_s) = \mu S_+(\omega_s)/\varepsilon_s = (\mu^2/\hbar\Gamma_2)\chi^{(1)}(\omega_s)$, and $\chi^{(1)}(\omega_s)$ is given by

$$\chi^{(1)}(\omega_s) = \frac{(\Sigma_4\theta_2 - \theta_1\theta_8)\Gamma_2}{\Sigma_1\Sigma_4 + \theta_1\theta_7} \tag{15}$$

where

$$\Pi_1 = \frac{\lambda^{'}}{\omega_{m1}^{'2} - i\gamma_{m1}\delta - \delta^2}, \Pi_2 = \frac{-2\omega_{m1}^2\beta}{\omega_{m1}^{'2} - i\gamma_{m1}\delta - \delta^2}, \Pi_3 = \frac{\lambda^{'}}{\omega_{m2}^{'2} - i\gamma_{m2}\delta - \delta^2}, \Lambda_1 = \frac{\Pi_4 - \Pi_2\Pi_3}{1 - \Pi_1\Pi_3},$$

$$\Pi_4 = \frac{-2\lambda\omega_{m1}\beta}{\omega_{m1}^{'2} - i\gamma_{m1}\delta - \delta^2}, \Lambda_2 = \frac{\Pi_2 - \Pi_1\Pi_4}{1 - \Pi_1\Pi_3}, \theta_1 = \frac{\Omega_p(2\Omega_p + \omega_{m1}\beta S_0\Lambda_2)}{\Gamma_1 - i\delta},$$

$$\theta_2 = \frac{S_0^*(2\Omega_p + \omega_{m1}\beta S_0\Lambda_2) - i\omega_0(\Gamma_1 - i\delta)}{\Gamma_1 - i\delta}, \theta_3 = \frac{\Omega_p(2\Omega_p + \omega_{m1}\beta S_0\Lambda_2^*)}{\Gamma_1 + i\delta},$$

$$\theta_4 = \frac{S_0(2\Omega_p + \omega_{m1}\beta S_0\Lambda_2^*)}{\Gamma_1 + i\delta}, \theta_5 = -\frac{\Omega_p(2\Omega_p + \omega_{m1}\beta S_0^*\Lambda_2^*)}{\Gamma_1 + i\delta}, \tag{16}$$

$$\theta_6 = \frac{S_0(2\Omega_p + \omega_{m1}\beta S_0^*\Lambda_2^*) - i\omega_0(\Gamma_1 + i\delta)}{\Gamma_1 + i\delta}, \theta_7 = -\frac{\Omega_p(2\Omega_p + \omega_{m1}\beta S_0^*\Lambda_2)}{\Gamma_1 - i\delta},$$

$$\theta_8 = \frac{S_0^*(2\Omega_p + \omega_{m1}\beta S_0^*\Lambda_2)}{\Gamma_1 - i\delta}, \Sigma_1 = i(\Delta_p^{'} - \delta) + \Gamma_2 + \theta_1, \Sigma_2 = i(\Delta_p^{'} + \delta) + \Gamma_2 + \theta_3,$$

$$\Sigma_3 = -i(\Delta_p^{'} - \delta) + \Gamma_2 - \theta_5, \Sigma_4 = -i(\Delta_p^{'} + \delta) + \Gamma_2 - \theta_7,$$

The imaginary and real parts of $\chi^{(1)}(\omega_s)$ indicate absorption and dispersion, respectively.

Due to the light group velocity as [44,45] $\upsilon_g = c/[n + \omega_s(dn/d\omega_s)]$, where $n \approx 1 + 2\pi\chi_{eff}^{(1)}$, then we obtain

$$\frac{c}{\upsilon_g} = 1 + 2\pi\,\mathrm{Re}\,\chi^{(1)}(\omega_s)_{\omega_s=\omega_{ex}} + 2\pi\omega_s\,\mathrm{Re}\left(\frac{d\chi^{(1)}(\omega_s)}{d\omega_s}\right)_{\omega_s=\omega_{ex}}. \tag{17}$$

It is obvious that the dispersion is steeply positive or negative, and the group velocity is significantly reduced or increased at $\mathrm{Re}\,\chi^{(1)}(\omega_s)_{\omega_s=\omega_{ex}}=0$. We further define the group velocity index n_g as

$$n_g=\frac{c}{\upsilon_g}-1=\frac{2\pi\omega_s\rho\mu^2}{\hbar\Gamma_2}\mathrm{Re}(\frac{d\chi^{(1)}(\omega_s)}{d\omega_s})_{\omega_s=\omega_{ex}}=\Gamma_2\Sigma\,\mathrm{Re}(\frac{d\chi^{(1)}(\omega_s)}{d\omega_s})_{\omega_s=\omega_{ex}} \tag{18}$$

where $\Sigma=2\pi\omega_s\rho\mu^2/\hbar\Gamma_2^2$. One can observe the slow light if $n_g>0$, and the superluminal light when $n_g<0$ [2].

3. Numerical results and discussion

We use the realistic hybrid QD-NR system to illustrate the numerical results [26]: the exciton relaxation rate $\Gamma_1=0.3$ GHz, the exciton dephasing rate $\Gamma_2=0.15$ GHz. The physical parameters of GaAs NR are $(\omega_{m1},m,Q)=(1.2\text{ GHz},5.3\times10^{-15}g,3\times10^4)$, where m and Q are the effective mass and quality factor of the NR, respectively. The decay rate of the NR is $\gamma_{m1}=\omega_{m1}/Q=40$ kHz, the coupling strength between QD and NR is $\beta=0.06$, and the frequency of another NR is $\omega_{m2}=\omega_{m1}$. We first investigate the probe absorption, i.e., the imaginary part ($\mathrm{Im}\,\chi^{(1)}$) of linear optical susceptibility, as a function of probe-exciton detuning $\Delta_s=\omega_s-\omega_{ex}$ on the condition of resonance (i.e., $\Delta_p=0$) for different coupling strength λ_1 of the two NRs as shown in Fig.2(a). In Fig.2(a), when the interaction of the NRs is $\lambda_1=0$, i.e., only one NR in the system and two sharp sideband peaks at both sides of the probe absorption spectrum just correspond to the frequency of the NR with frequency $\omega_{m1}=1.2$ GHz, . The physical origin of the phenomenon has been demonstrated in a coupled NR system [16] with the dressed states theory. If the coupling strength $\lambda_1\neq0$, such as $\lambda_1=0.05\omega_{m1}$, we find four sharp sideband peaks appear in the probe absorption spectrum, where the left two peaks mean the process of amplification and the right two peaks mean the process of absorption as shown the red curve in Fig.2(a). In addition, the left two sharp sideband peaks locate at $-\omega_{m1}-\lambda_1$ and $-\omega_{m1}+\lambda_1$, i.e., $-1.05\omega_{m1}$ and $-0.95\omega_{m1}$, respectively, while the right two sharp sideband peaks locate at $\omega_{m1}-\lambda_1$ and $\omega_{m1}+\lambda_1$, i.e., $0.95\omega_{m1}$ and $1.05\omega_{m1}$, respectively. That is to say the four sharp sideband peaks locate at $\pm\omega_{m1}\pm\lambda_1$ and $\pm\omega_{m1}\mp\lambda_1$, respectively. When we increasing the coupling strength λ_1 from $\lambda_1=0.05\omega_{m1}$ to $\lambda_1=0.1\omega_{m1}$, the four sharp sideband peaks locate at $\pm1.1\omega_{m1}$ and $\pm0.9\omega_{m1}$ which still correspond to $\pm\omega_{m1}\pm\lambda_1$ and $\pm\omega_{m1}\mp\lambda_1$ as shown the blue curve in Fig.2(a). Fig.2(b) and Fig.2(c) show the details of the process of the left amplification and the right absorption as in Fig.2(a), respectively. Figure 2(d) presents the splitting of the two sharp sideband peaks (both the left amplification process and the right absorption process) as a function of the normalized coupling strength λ_1/ω_{m1} of the two NRs. It is obvious that the splitting distance of the probe absorption spectrum increases linearly with increasing the coupling strength λ_1. Therefore, the plots may provide a method to roughly measure the coupling strength λ_1 of the two NRs via the splitting in the optical spectrum.

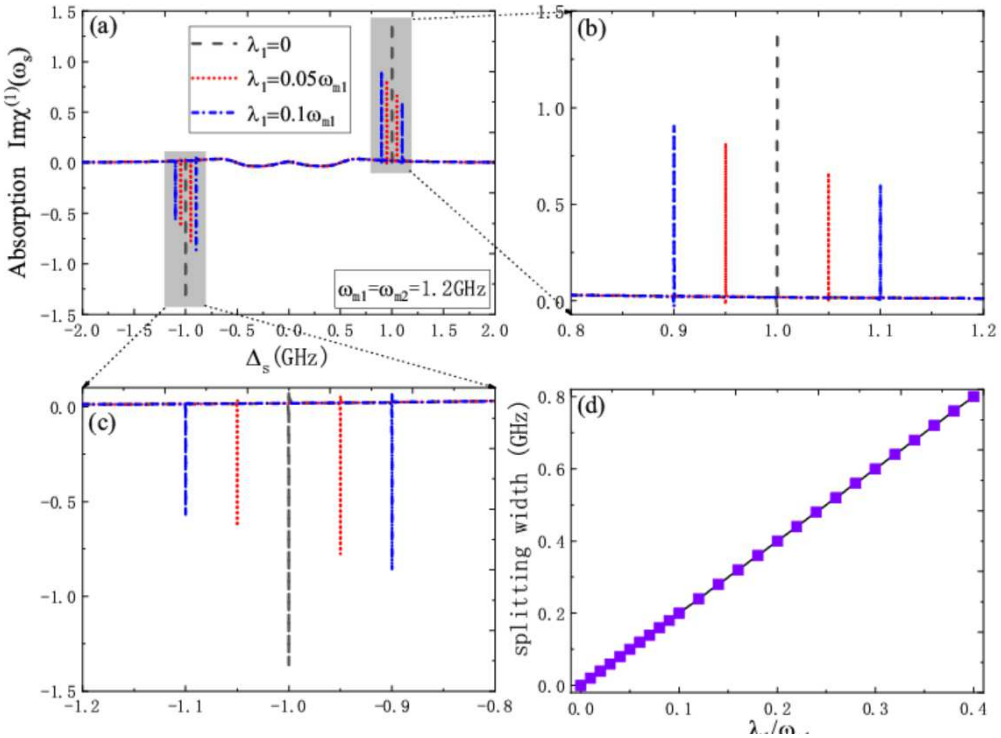

Fig. 2. (a) The probe absorption as a function of probe-exciton detuning Δ_s under the condition of resonance ($\Delta_p = 0$) for different coupling strengths λ_1 under the same resonator frequencies. (b) The details of the amplification for the right peaks of the absorption spectra. (c) The details of the amplification for the left peaks of the absorption spectra. (d) The splitting of the two sharp sideband peaks as a function of the normalized coupling strength λ_1/ω_{m1}.

Secondly, switching the detuning Δ_p from the resonance ($\Delta_p = 0$) to the red sideband ($\Delta_p = \omega_{m1}$), we study the probe absorption spectrum as a function of Δ_s for different coupling strength λ_1 at fixed exciton-resonator coupling $\beta = 0.06$ with the same frequencies of the NRs as shown in Fig.3(a). In Fig.3(a), when the coupling strength $\lambda_1 = 0$ (the black curve), the absorption spectrum splits into two peaks, which is analogous to the Rabi splitting of TLSs in quantum optics and has a zero absorption point at $\Delta_s = 0$. The physical origin is due to mechanically induced coherent population oscillation which makes a deep hole $\Delta_s = 0$ in the probe absorption spectrum, which has been demonstrated in a QD-NR system [16]. Then we consider the coupling strength $\lambda_1 = 0.05\omega_{m1}$ (the red curve in Fig.3(a)), we find that three peaks appear in the absorption spectrum, and more remarkable the peak at $\Delta_s = 0$ in the case of $\lambda_1 = 0$ splits into two peaks under the case of $\lambda_1 \neq 0$. In addition, the width of the two peaks around $\Delta_s = 0$ is $2\lambda_1$. With increasing the coupling strength λ_1, such as $\lambda_1 = 0.1\omega_{m1}$ (the blue curve in Fig.3(a)), the splitting width is more obvious, and the two peaks around $\Delta_s = 0$ accurately locate at $\pm\lambda_1/\omega_{m1}$. In Fig.3(b), we show the dispersion, i.e., the real part of linear optical susceptibility $\mathrm{Re}\,\chi^{(1)}$, under three different coupling strength λ_1 for $\beta = 0.06$ with the resonator frequencies $\omega_{m2} = \omega_{m1}$. When the coupling strength λ_1 changes from $\lambda_1 = 0$ to $\lambda_1 \neq 0$, the evolution of the process of the slope around $\Delta_s = 0$ experiences the

conversion from positive to negative. As we know, the positive steep slope of dispersion will induce the group velocity index $n_g > 0$, then the slow light phenomenon will appear in system. While if the dispersion shows the negative steep slope, the group velocity index $n_g < 0$, and the fast light will achieve. Combining with Fig.3(a) and Fig.3(b), no matter what regimes induce the zero absorption, once a transparency window appear in the probe absorption spectra, the remarkable phenomena of slow light or fast light can appear in the hybrid system. When the transparency appear in the absorption, the slope around transparency window of the dispersion will experience the conversion between the positive to negative. Figure 3(c) plots the group velocity index n_g versus the Rabi frequency Ω_p^2 for the coupling strength $\lambda_1 = 0$ under the red sideband $\Delta_p = \omega_{m1}$, and one can see that the group velocity index n_g is positive representing the slow light effect. However, if the coupling strength $\lambda_1 \neq 0$, the group velocity index n_g manifests the fast light effect as shown in Fig.3(d). Although the fast light effect was demonstrated in a carbon nanotube resonator [36] which need the condition of resonance ($\Delta_p = 0$), in our hybrid system, the fast light effect can even achieve still at the red sideband $\Delta_p = \omega_{m1}$ by controlled the coupling of the two NRs.

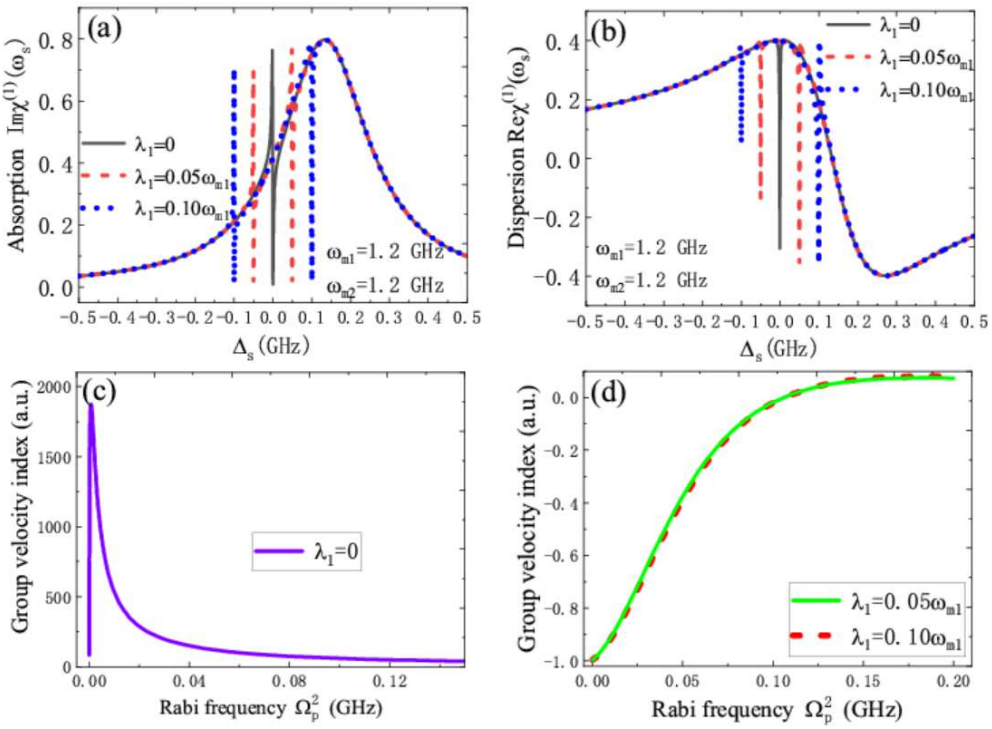

Fig. 3. (a) The probe absorption as a function of Δ_s under the detuning ($\Delta_p = \omega_{m1}$) for different coupling strengths λ_1 under the same resonator frequencies. (b) the dispersion under three different coupling strengths λ_1 for with the resonator frequencies $\omega_{m2} = \omega_{m1}$. (c) The group velocity index n_g versus the Rabi frequency Ω_p^2 under λ_1=0. (d) The group velocity index n_g versus the Rabi frequency Ω_p^2 under $\lambda_1 \neq 0$.

Getting back to Fig.2(a), if the coupling strength $\lambda_1 \neq 0$, the probe absorption spectra present three modes splitting manifesting the phenomenon of double Fano resonance, so we further investigate the double Fano resonance under different parameter regimes. In Fig.4(a), we first present the absorption profiles as a function of the probe detuning $\Delta_s = 0$ at the fixed coupling strength ($\lambda_1 = 0.1\omega_{m1}$) and the same frequency of the NRs ($\omega_{m2} = \omega_{m1} = 1.2$ GHz) for different pump detuning Δ_p. It is obvious that the double-Fano resonances appear in the absorption spectra, where the right Fano resonance is induced by the coupling between exciton and a NR making quantum interference between the NR and the two optical fields via the exciton as $\delta = \omega_{m1}$, and the left Fano resonance come from the coupling between the two NRs. In addition, with increasing the detuning Δ_p from $\Delta_p = 0.9\omega_{m1}$ to $\Delta_p = 1.1\omega_{m1}$ (Fig.4(a) to Fig.4(c)), the right Fano resonance move to the right. Secondly, we fix the red sideband $\Delta_p = \omega_{m1}$ and plot the absorption spectra as a function of detuning Δ_s for several different resonator frequencies at the coupling strengths $\lambda_1 = 0.1\omega_{m1}$ as shown in Fig.4(d) to Fig.4(f). From Fig.4(d) to Fig.4(f), we find that if $\omega_{m2} = \omega_{m1}$, double Fano resonance can also appear in the absorption spectra and two sharp peaks locate at $\pm\lambda_1/\omega_{m1}$ as shown in Fig.4(e). When the condition of the frequencies for the two NRs satisfies $\omega_{m1} > \omega_{m2}$, we obtain the absorption profile moves to the left as shown in Fig.4(d), if $\omega_{m1} < \omega_{m2}$ the absorption profile moves to the right as shown in Fig.4(f). While in the both case the Lorentz peak almost unmoved from beginning to end.

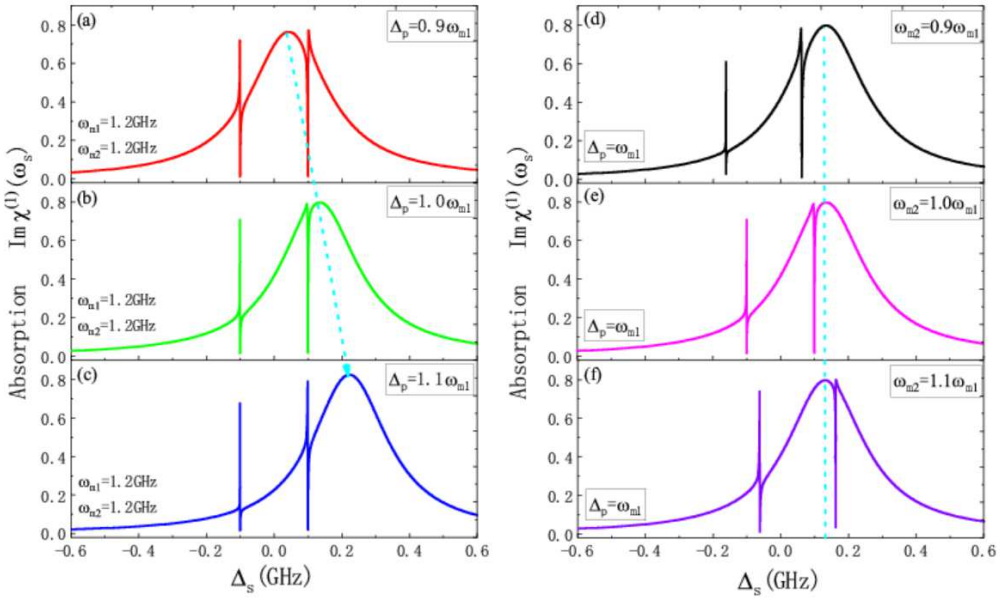

Fig. 4. (a)-(c) The probe absorption for different the exciton-pump field detuning Δ_p with the same frequencies $\omega_{m2} = \omega_{m1}$. (d)-(f) The probe absorption as a function of Δ_s under the detuning ($\Delta_p = \omega_{m1}$) for different resonator frequencies.

Therefore, we also investigate the double-Fano resonances that induce the coherent optical propagation properties as shown in Fig.5. In Fig.5(a), we plot the group velocity index n_g versus the Rabi frequency Ω_p^2 for different detuning Δ_p with the same resonator frequencies

of the two NRs at fixed coupling strength $\lambda_1 = 0.1\omega_{m1}$. We can find that the group velocity index n_g experiences the switch from fast light to slow light with increasing the Rabi frequency Ω_p^2. In addition, if $\Delta_p < \omega_{m1}$, the group velocity index n_g experiences the processes from small to large in the fast light and then reach to slow light. In Fig.5(a), we show the group velocity index n_g as a function of the Rabi frequency Ω_p^2 for different resonator frequencies at $\Delta_p = \omega_{m1}$ for fixed coupling strength $\lambda_1 = 0.1\omega_{m1}$. With increasing the resonator frequency ω_{m2} from $\omega_{m2} = 0.9\omega_{m1}$ to $\omega_{m2} = 1.1\omega_{m1}$, the group velocity index n_g experiences conversion from fast light to slow light. Thus, with controlling the detuning regime and the coupling of the two NRs, the fast-to-slow light can be achieved straightforward in the hybrid system.

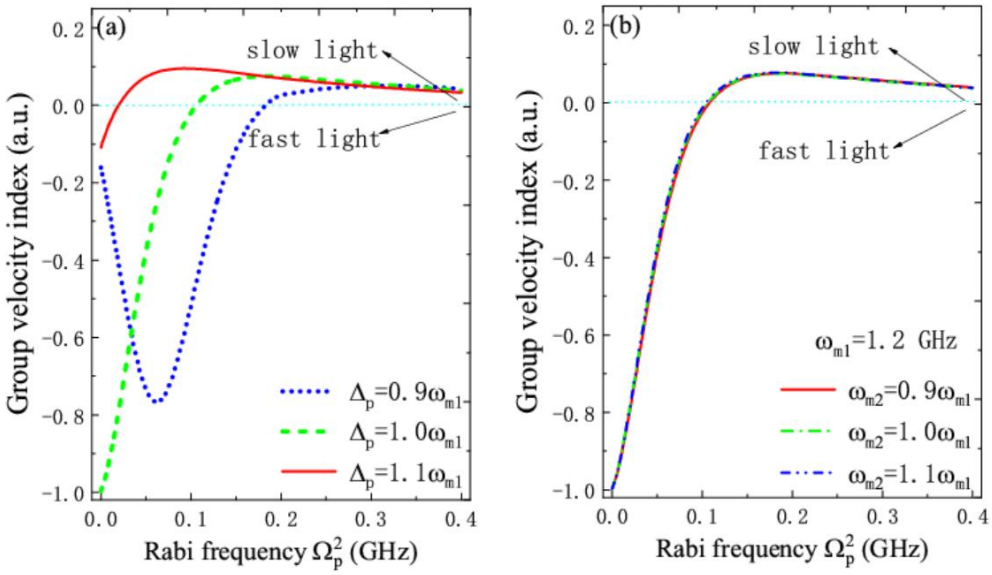

Fig. 5. (a) The group velocity index n_g versus the Rabi frequency Ω_p^2 for several different Δ_p. (b) The group velocity index n_g versus the Rabi frequency Ω_p^2 for several different resonator frequencies.

4. Conclusion

In conclusion, we have proposed a hybrid NR system consisting of a suspended NR with an embedded QD driven by a pump field and a probe field is coupled to another NR with different frequencies via the Coulomb interaction, and investigated the absorption spectra of the probe field both under the conditions of the resonance ($\Delta_p = 0$) and off-resonance ($\Delta_p = \omega_{m1}$). In the situation of resonance, the sharp peaks in the absorption spectra depend on the interaction between the NRs, which display a method to determine the coupling strength of the two NRs. When in the off-resonance, we theoretically studied the double Fano resonance, and the positions and the shape of the double Fano line shapes are closely related to the detuning and the coupling strengths between the NRs. Moreover, the narrow transparency window in the probe transmission and the corresponding rapid phase dispersion allow for reaching the slow light effect. We have shown that the group velocity index of the probe field can be effectively tuned by the coupling strengths of the NRs and the pump detuning, and even obtain the conversion from slow light to fast light in hybrid NR system.

Abbreviations

NR: Nanomechanical resonator; QD: Quantum dot; TLS: two-level system; QD-NR: Quantum dot- nanomechanical resonator; Q: quality factor.

Acknowledgements

The authors gratefully acknowledge support from the National Natural Science Foundation of China (Nos:11647001 and 11804004); Project funded by China Postdoctoral Science Foundation (No:2020M681973); Anhui Provincial Natural Science Foundation (No:1708085QA11).

Funding

Hua-Jun Chen is supported by National Natural Science Foundation of China (Nos:11647001 and 11804004); Project funded by China Postdoctoral Science Foundation (No:2020M681973); Anhui Provincial Natural Science Foundation (No:1708085QA11).

Availability of data and materials

The QD-NR system is demonstrated in Ref.[26] and the Coulomb interaction please see Ref.[33–35].

Authors' contributions

HJC finished the main work of this paper, including conceiving of the idea, deducing the formulas, plotting the figures, and drafting the manuscript. All authors are involved in revising the manuscript. All authors read and approved the final manuscript.

Competing interests

The authors declare that they have no competing interests.

References

1. M. O. Scully and M. S. Zubairy, "Playing tricks with slow light," Science, **301**(5630), 181-182 (2003).
2. R. W. Boyd and D. J. Gauthier, "Controlling the velocity of light pulses," Science **326**(5956), 1074-1077 (2009).
3. L. V. Hau, S. E. Harris, Z. Dutton, and C. H. Behroozi, "Light speed reduction to 17 metres per second in an ultracold atomic gas," Nature **397**, 594-598 (1999).
4. D. Budker, D. F. Kimball, S. M. Rochester, and V. V. Yashchuk, "Nonlinear magneto-optics and reduced group velocity of light in atomic vapor with slow ground state relaxation," Phys. Rev. Lett. **83**(9), 1767 (1999).
5. M. Fleischhauer, A. Imamoglu, J. P. Marangos, "Electromagnetically induced transparency: Optics in coherent media," Rev. Mod. Phys. **77**(2), 633 (2005).
6. V. P. Kalosha, L. Chen, and X. Bao, "Slow and fast light via SBS in optical fibers for short pulses and broadband pump," Opt. Express **14**(26), 12693-12703 (2006).
7. V. I. Kovalev, N. E. Kotova, and R. G. Harrison, "Slow light in stimulated Brillouin scattering: on the influence of the spectral width of pump radiation on the group index: reply," Opt. Express **18**(2), 1791-1793 (2010).
8. M. S. Bigelow, N. N. Lepeshkin, and R. W. Boyd, "Observation of ultraslow light propagation in a ruby crystal at room temperature," Phys. Rev. Lett. **90**(11), 113903 (2003).
9. S. Zhang, D. A. Genov, Y. Wang, M. Liu, and X. Zhang, "Plasmon-induced transparency in metamaterials," Phys. Rev. Lett. **101**(4), 047401 (2008).
10. A. E. Miroshnichenko, S. Flach, Y.S. Kivshar, "Fano resonances in nanoscale structures," Rev. Mod. Phys. **82**(3), 2257 (2010)
11. B. Luk'yanchuk, N. I. Zheludev, S. A. Maier, N. J. Halas, P. Nordlander, H. Giessen, C. T. Chong, "The Fano resonance in plasmonic nanostructures and metamaterials," Nat. Mater. **9**, 707-715 (2010)
12. C. Wu, A. B. Khanikaev, and G. Shvets, "Broadband slow light metamaterial based on a double-continuum Fano resonance," Phys. Rev. Lett. **106**(10), 107403 (2011).
13. M. Poot, H. S. J. van der Zant, "Mechanical systems in the quantum regime," Phys. Rep, **511**(5), 273-335 (2013).
14. B. Lassagne, Y. Tarakanov, J. Kinaret, D. Garcia-Sanchez, A. Bachtold1, "Coupling mechanics to charge transport in carbon nanotube mechanical resonators," Science, **325**(5944), 1107-1110 (2009)
15. J. Tamayo, P. M. Kosaka, J. J. Ruz, A. S. Paulo, and M. Calleja, "Biosensors based on nanomechanical systems," Chem. Soc. Rev, **42**, 1287-1311 (2013).

16. J. J. Li, K. D. Zhu, ”All-optical mass sensing with coupled mechanical resonator systems,” Phys. Rep, **525**(3), 223-254 (2013).
17. M. D. LaHaye, O. Buu, B. Camarota, K. C. Schwab, ”Approaching the quantum limit of a nanomechanical resonator,” Science, **304**(2556), 74-77 (2004).
18. D. Rugar, R. Budakian, H. J. Mamin, B. W. Chui, ”Single spin detection by magnetic reso-nance force microscopy,” Nature, **430**, 329-332 (2004).
19. M. D. LaHaye, J. Suh, P. M. Echternach, K. C. Schwab, and M. L. Roukes, ”Nanomechanical measurements of a superconducting qubit,” Nature **459**, 960 (2009).
20. D. Hunger, S. Camerer, T. W. Hansch, D. Konig, J. P. Kotthaus, J. Reichel, and P. Treutlein, ”Resonant coupling of a Bose–Einstein condensate to a micromechanical oscillator,” Phys. Rev. Lett. **104**(14), 143002 (2010).
21. O. Arcizet, V. Jacques, A. Siria, P. Poncharal, P. Vincent, and S. Seidelin, ”A single nitrogen-vacancy defect coupled to a nanomechanical oscillator,” Nature Phys. **7**, 879-883 (2011).
22. S. Kolkowitz, A. C. B. Jayich, Q. P. Unterreithmeier1, S. D. Bennett, P. Rabl, J. G. E. Harris, M. D. Lukin, ”Coherent sensing of a mechanical resonator with a single-spin qubit,” Science **335**(6076), 1603-1606 (2012).
23. J.-M. Pirkkalainen, S. U. Cho, Jian Li, G. S. Paraoanu, P. J. Hakonen, and M. A. Sillanpaa, ”Hybrid circuit cavity quantum electrodynamics with a micromechanical resonator,” Nature **494**, 211-215 (2013).
24. A. D. O’Connell, M. Hofheinz, M. Ansmann, R. C. Bialczak, M. Lenander, E. Lucero, M. Neeley, D. Sank, H. Wang, M. Weides, J. Wenner, John M. Martinis, and A. N. Cleland, ”Quantum ground state and single-phonon control of a mechanical resonator,” Nature **464**, 697-703 (2010).
25. T. A. Palomaki, J. W. Harlow, J. D. Teufel, R. W. Simmonds, and K. W. Lehnert, ”Coherent state transfer between itinerant microwave fields and a mechanical oscillator,” Nature **495**, 210 (2013).
26. I. Wilson-Rae, P. Zoller, A. Imamoglu, "Laser cooling of a nanomechanical resonator mode to its quantum ground state,” Phys. Rev. Lett. **92**(7), 075507 (2004),
27. S. D. Bennett, L. Cockins, Y. Miyahara, P. Grutter, and A. A. Clerk, ”Strong electromechanical coupling of an atomic force microscope cantilever to a quantum dot,” Phys. Rev. Lett. **104**(1), 017203 (2010).
28. I. Yeo, P.-L. de Assis, A. Gloppe, E. Dupont-Ferrier, P. Verlot, N. S. Malik, E. Dupuy, J. Claudon, J.-M. Gerard, A. Auffeves, G. Nogues, S. Seidelin, J.-P. Poizat, O. Arcizet, and M. Richard, ”Strain-mediated coupling in a quantum dot-mechanical oscillator hybrid system,” Nat. Nanotechnol, **9**, 106-110 (2014).
29. K. C. Schwab and M. L. Roukes, ”Putting mechanics into quantum mechanics,” Phys. Today **58**(7), 36-42 (2005).
30. Y. J. Wang, M. Eardley, S. Knappe, J. Moreland, L. Hollberg, and J. Kitching, ”Magnetic resonance in an atomic vapor excited by a mechanical resonator,” Phys. Rev. Lett. **97**(22), 227602 (2006).
31. Y. T. Yang, C. Callegari, X. L. Feng, K. L. Ekinci, and M. L. Roukes, ”Zeptogram-scale nanomechanical mass sensing,” Nano. Lett. **6**(4), 583 (2006).
32. K. Fang, M. Matheny, X. Luan, and O. Painter, ”Optical transduction and routing of microwave phonons in cavity-optomechanical circuits,” Nat. Photon. **10**, 489 (2016).
33. Q. Wang, J. Q. Zhang, P. C. Ma, C. M. Yao, and M. Feng, ”Precision measurement of the environmental temperature by tunable double optomechanically induced transparency with a squeezed field,” Phys. Rev. A **91**(6), 063827 (2015).
34. W. K. Hensinger, D. W. Utami, H. S. Goan, K. Schwab, C. Monroe, and G. J. Milburn, ”Ion trap transducers for quantum electromechanical oscillators,” Phys. Rev. A **72**(4), 041405(R) (2005).
35. Z. Qian, M. M. Zhao, B. P. Hou, and Y. H. Zhao, ”Tunable double optomechanically induced transparency in photonically and phononically coupled optomechanical systems,” Opt. Express, **25**(26), 33097-33112 (2017).
36. J. J. Li and K. D. Zhu, ”Tunable slow and fast light device based on a carbon nanotube resonator,” Opt. Express, **20**(6), 5840-5848 (2012).
37. P. C. Ma, J. Q. Zhang, Y. Xiao, M. Feng, and Z. M. Zhang, ”Tunable double optomechanically induced transparency in an optomechanical system,” Phys. Rev. A **90**(4), 043825 (2014).
38. Q. Yang, B. P. Hou, D. G. Lai, ”Local modulation of double optomechanically induced transparency and amplification,” Optics Express, **25**(9), 9697-9711 (2017).
39. A. Zrenner, E. Beham, S. Stufler, F. Findeis, M. Bichler, G. Abstreiter, ”Coherent properties of a two-level system based on a quantum-dot photodiode,” Nature **418**, 612-614 (2002).
40. S. Stufler, P. Ester, A. Zrenner, M. Bichler, ”Quantum optical properties of a single InxGa1xAs-GaAs quantum dot two-level system,” Phys. Rev. B **72**(12), 121301 (2005).
41. Walls, D. F. and Milburn, G. J. Quantum Optics (Springer, 1994) p. 245
42. G. S. Agarwal, S. Huang, ”Electromagnetically induced transparency in mechanical effects of light,” Phys. Rev. A **81**(4), 041803 (2010).
43. R. W. Boyd, Nonlinear Optics (Academic, San Diego, California, 1992), p. 225.
44. S. E. Harris, J. E. Field, A. Kasapi, ”Dispersive properties of electromagnetically induced transparency,” Phys. Rev. A **46**(1), R29 (1992).
45. R. S. Bennink, R. W. Boyd, C. R. Stroud, V. Wong, ”Enhanced self-action effects by electromagnetically induced transparency in the two-level atom,” Phys. Rev. A **63**(3), 033804 (2001).
46. R. W. Boyd and D. J. Gauthier, ”Controlling the velocity of light pulses,” Science **326**(5956), 1074 (2009).

Figures

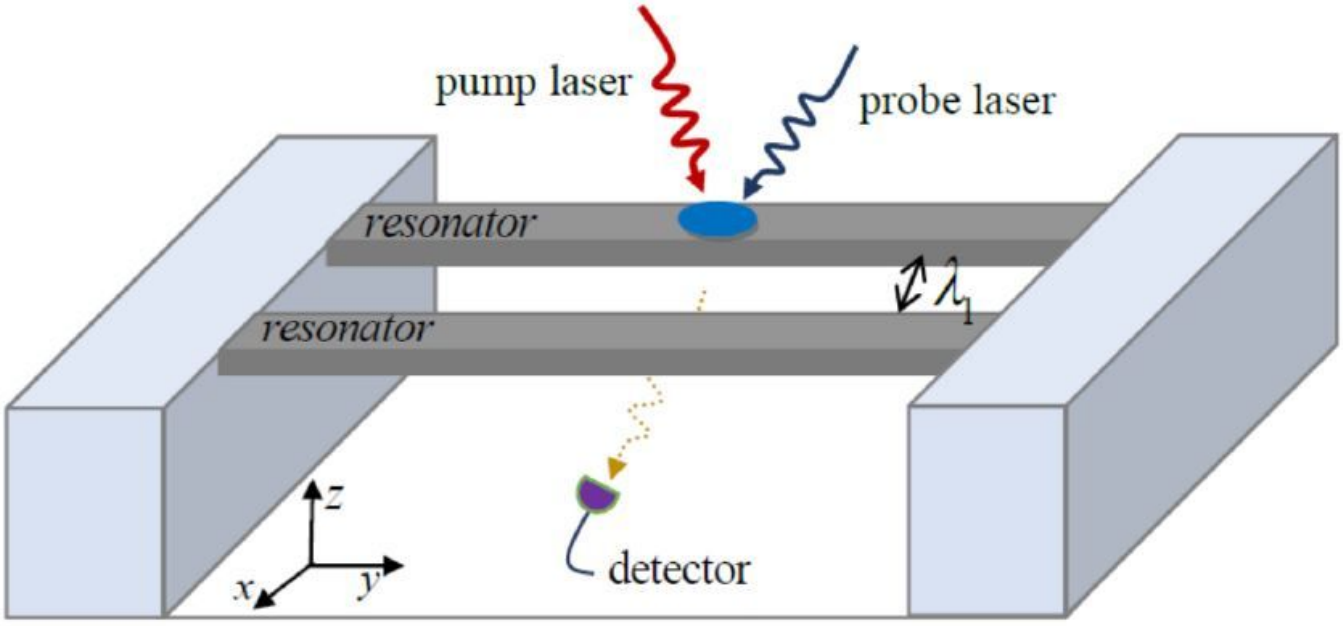

Figure 1

"Please see the Manuscript PDF file for the complete figure caption".

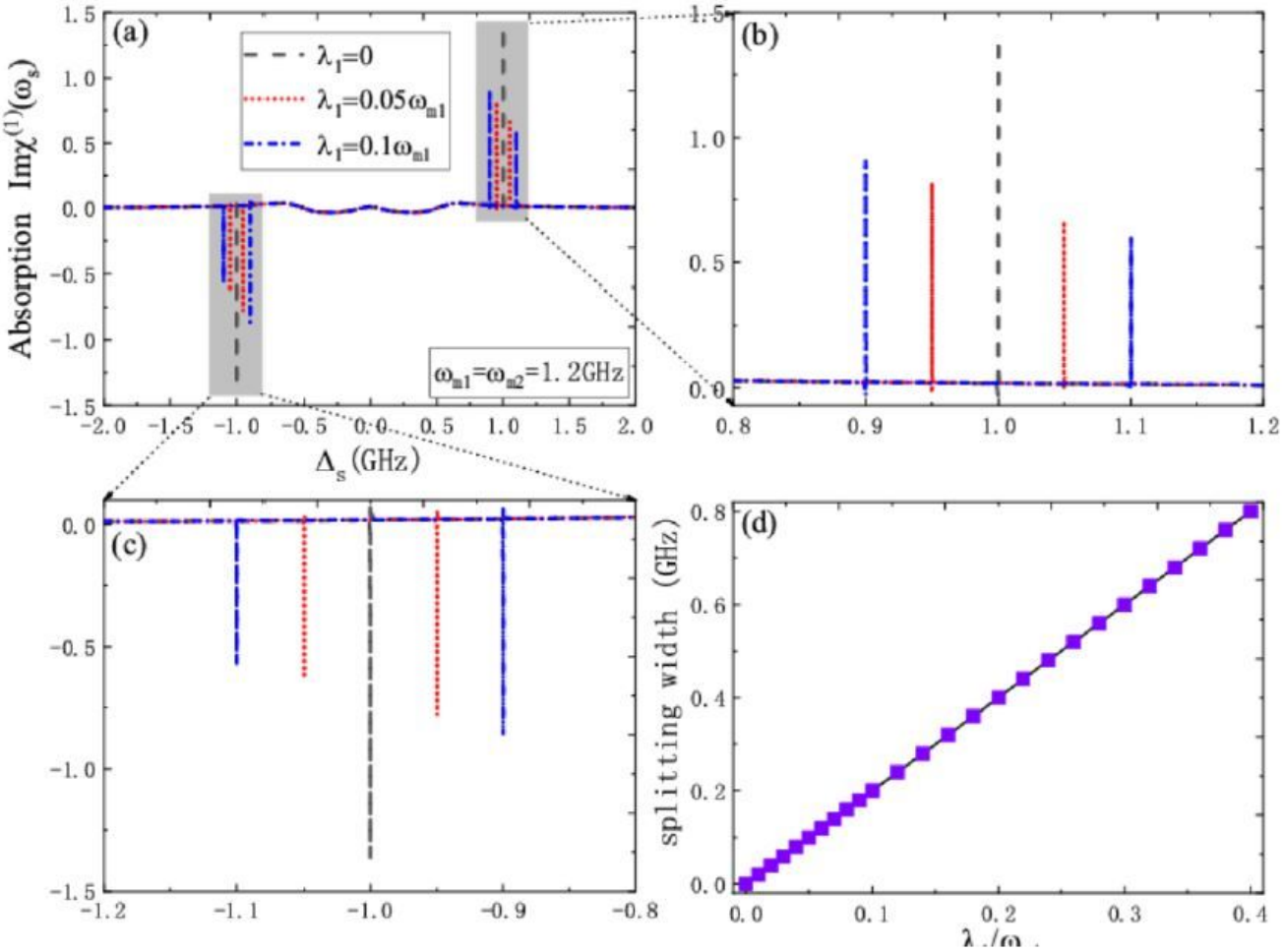

Figure 2

"Please see the Manuscript PDF file for the complete figure caption".

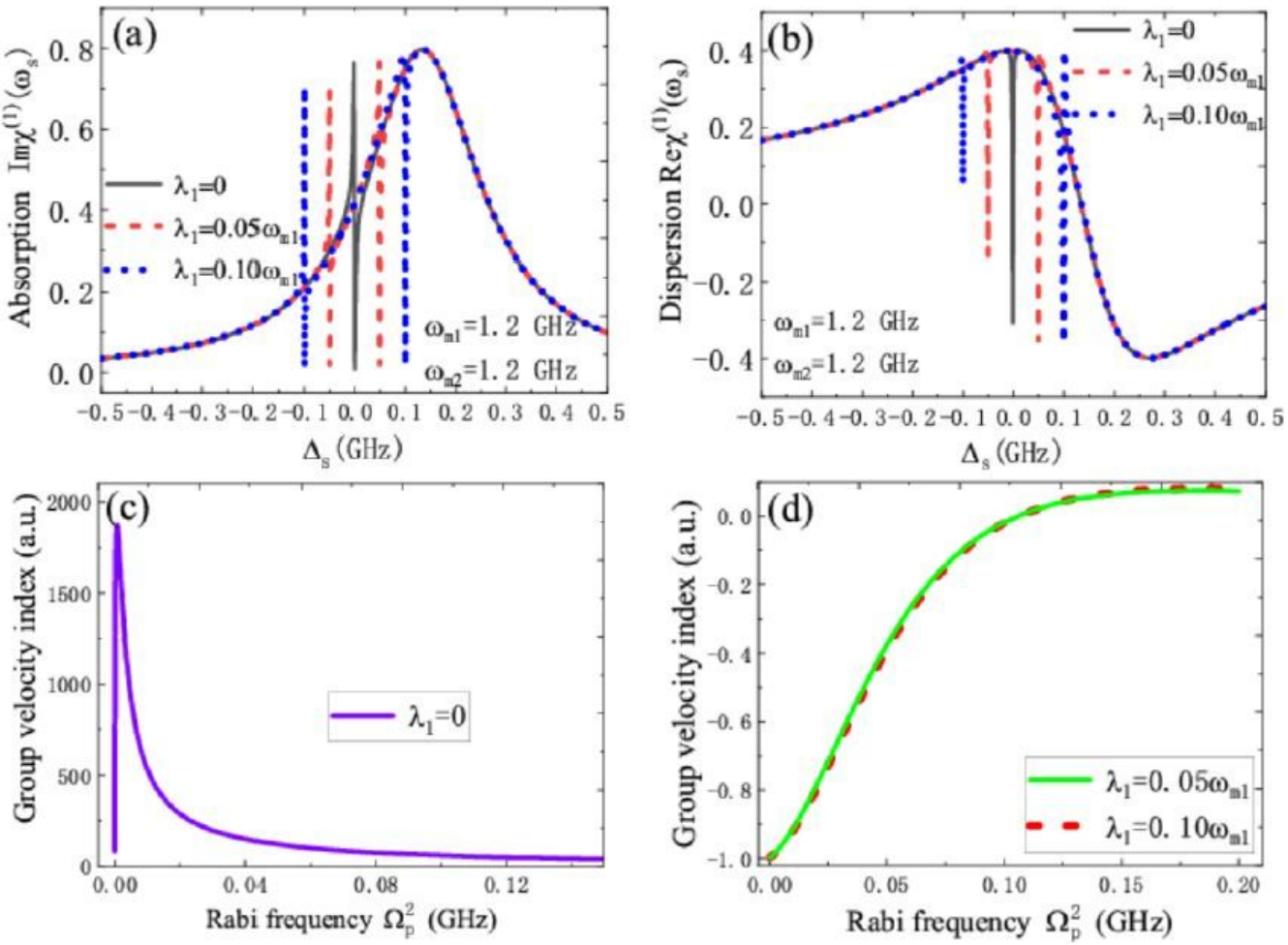

Figure 3

"Please see the Manuscript PDF file for the complete figure caption".

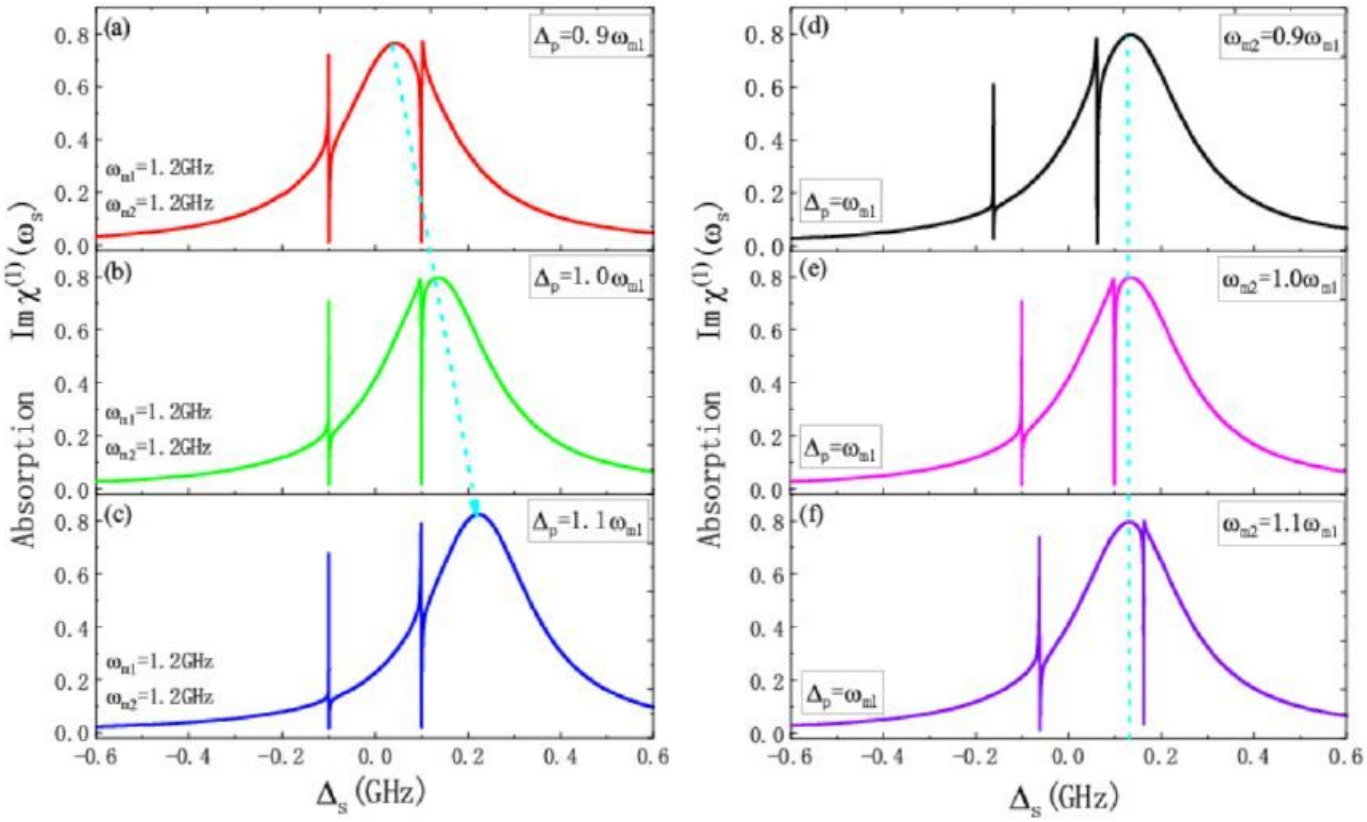

Figure 4

"Please see the Manuscript PDF file for the complete figure caption".

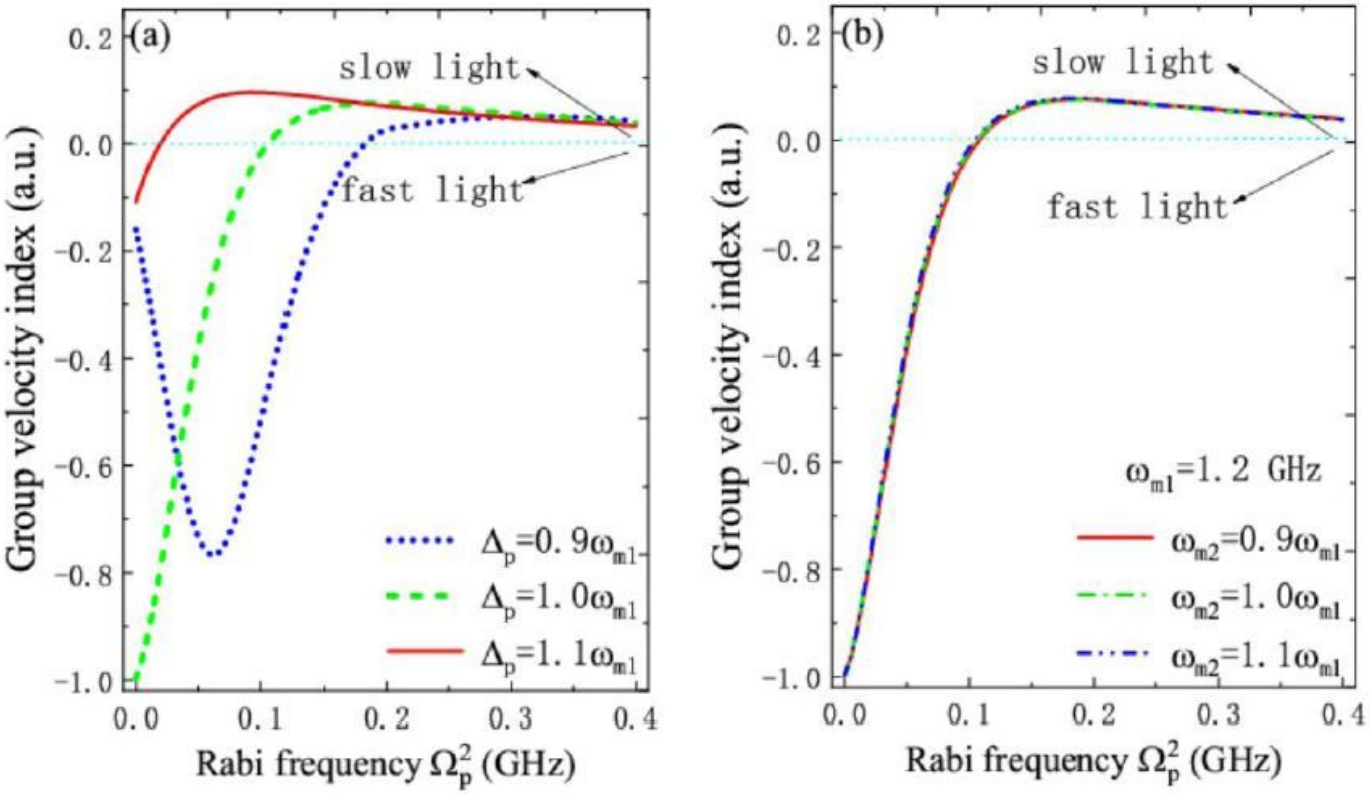

Figure 5

"Please see the Manuscript PDF file for the complete figure caption".